

# High temperature-gradient refractive index liquid crystals

Jun Li, Sebastian Gauza, and Shin-Tson Wu

School of Optics/CREOL, University of Central Florida, Orlando, Florida 32816, USA

[swu@mail.ucf.edu](mailto:swu@mail.ucf.edu)

<http://lcd.creol.ucf.edu>

**Abstract:** We have analyzed the physical origins of the temperature gradient of the ordinary refractive index ( $dn_o/dT$ ) of liquid crystals. To achieve a large  $dn_o/dT$ , high birefringence and low clearing temperature play crucial roles. Based on these simple guidelines, we formulated two exemplary liquid crystal mixtures, designated as UCF-1 and UCF-2, and compared their physical properties with a commonly used commercial liquid crystal compound 5CB. The  $dn_o/dT$  of UCF-1 is ~4X higher than that of 5CB at room temperature.

©2004 Optical Society of America

**OCIS codes:** (160.3710) Liquid crystals; (230.2090) Electro-optical devices; (190.4400) Nonlinear optics

---

## References and links

1. E. H. Stupp and M. S. Brennessoltz, *Projection Displays* (Wiley, New York, 1998).
2. S. T. Wu and D. K. Yang, *Reflective Liquid Crystal Displays* (Wiley, New York, 2001).
3. I. C. Khoo and S. T. Wu, *Optics and Nonlinear Optics of Liquid Crystals* (World Scientific, Singapore, 1993).
4. M. Warengem, J. F. Henninot, and G. Abbate, "Non linearly induced self waveguiding structure in dye doped nematic liquid crystals confined in capillaries," *Opt. Express* **2**, 483-490 (1998).  
<http://www.opticsexpress.org/abstract.cfm?URI=OPEX-2-12-483>
5. M. Warengem, J. F. Henninot, F. Derrin, and G. Abbate, "Thermal and orientational spatial optical solitons in dye-doped liquid crystals," *Mol. Cryst. Liq. Cryst.* **373**, 213-225 (2002).
6. M. Peccianti and G. Assanto, "Signal readdressing by steering of spatial solitons in bulk nematic liquid crystals," *Opt. Lett.* **26**, 1690-1692 (2001).
7. M. Peccianti, A. De Rossi, G. Assanto, A. De Luca, C. Umeton, and I.C. Khoo, "Electrically assisted self-confinement and waveguiding in planar nematic liquid crystal cells," *Appl. Phys. Lett.* **77**, 7-9 (2000).
8. J. D. Jackson, *Classical Electrodynamics* (Wiley, New York, 1962).
9. M. F. Vuks, "Determination of the optical anisotropy of aromatic molecules from the double refraction of crystals," *Opt. Spektrosk.* **20**, 644-647 (1966).
10. J. Li and S. T. Wu, "Extended Cauchy equations for the refractive indices of liquid crystals," *J. Appl. Phys.* **95**, 896-901 (2004).
11. J. Li, S. Gauza, S. T. Wu, "Temperature effect on liquid crystal refractive indices," *J. Appl. Phys.* (July 1, 2004).
12. S. T. Wu, "Birefringence dispersions of liquid crystals," *Phys. Rev. A* **33**, 1270-1274 (1986).
13. I. Haller, "Thermodynamic and static properties of liquid crystals" *Prog. Solid State Chem.* **10**, 103-110 (1975).
14. S. T. Wu and K. C. Lim, "Absorption and scattering measurements of nematic liquid crystals," *Appl. Opt.* **26**, 1722-1727 (1987).
15. S. Gauza, H. Wang, C. H. Wen, S. T. Wu, A. J. Seed and R. Dąbrowski, "High birefringence isothiocyanato tolane liquid crystals," *Jpn. J. Appl. Phys. Part 1*, **42**, 3463-3466 (2003).
16. A. Spadto, R. Dąbrowski, M. Filipowicz, Z. Stolarz, J. Przedmojski, S. Gauza, Y. H. Fan, S. T. Wu, "Synthesis, mesomorphic and optical properties of isothiocyanatotolanes," *Liq. Cryst.* **30**, 191-198 (2003).
17. L. Pohl and U. Finkenzeller, *Liquid Crystals: Applications and Uses* (World Scientific, Singapore, 1990), Chap. 4.

## 1. Introduction

Besides displays [1, 2], liquid crystal (LC) is also a useful medium for nonlinear optics [3]. For examples, laser induced thermal [4, 5] and orientational [6, 7] effects in dye-doped liquid crystal (LC) are fundamentally interesting and practically useful phenomena. If a LC exhibits a large temperature-gradient refractive index, then the required laser intensity for triggering the nonlinear optical effects to occur is reduced. An aligned LC layer exhibits two refractive indices: extraordinary ( $n_e$ ) and ordinary ( $n_o$ ). For most of the LC materials known so far, the temperature gradient of  $n_e$  is negative. On the other hand, the temperature gradient of  $n_o$  could change from negative to positive, depending on the LC material and operating temperature. Some commercial LCs, e.g., Merck E7, exhibit a negative  $dn_o/dT$  at room temperature, while 5CB (4-cyano-4-n-pentylbiphenyl) exhibits a positive  $dn_o/dT$ . It is important to develop guidelines for designing LC mixtures with a large  $dn_o/dT$  at room temperature.

In this paper, we analyze the factors affecting the  $dn_o/dT$  of a LC material. We find that high birefringence and low clearing temperature are the two crucial parameters for achieving a large  $dn_o/dT$ . However, these two requirements are often conflicting to each other. A high birefringence LC usually exhibits high melting and clearing temperatures. We have found some low temperature high birefringence compounds and successfully formulated two experimental LC mixtures, designated as UCF-1 and UCF-2. The  $dn_o/dT$  of UCF-1 is ~4X higher than that of 5CB at room temperature.

## 2. Theory

The classical Clausius-Mossotti equation correlates the dielectric constant ( $\epsilon$ ) of an isotropic media with molecular polarizability ( $\alpha$ ) and molecular packing density ( $N$ ) as follows [8]:

$$\frac{\epsilon - 1}{\epsilon + 2} = \frac{4\pi}{3} N\alpha. \quad (1)$$

In the optical frequencies, we substitute  $\epsilon = n^2$  and obtain the Lorentz-Lorenz equation [8]:

$$\frac{n^2 - 1}{n^2 + 2} = \frac{4\pi}{3} N\alpha. \quad (2)$$

For an anisotropic LC, there are two principal refractive indices:  $n_e$  (extraordinary ray) and  $n_o$  (ordinary ray). Each refractive index is determined by its corresponding molecular polarizabilities,  $\alpha_e$  and  $\alpha_o$ . Vuks [9] modified the Lorentz-Lorenz equation by replacing  $\langle n^2 \rangle = (n_e^2 + 2n_o^2)/3$  in the denominator and obtained the following equation for anisotropic media:

$$\frac{n_{e,o}^2 - 1}{\langle n^2 \rangle + 2} = \frac{4\pi}{3} N\alpha_{e,o}. \quad (3)$$

Based on Vuks model, the temperature-dependent LC refractive indices can be expressed by the average refractive index  $\langle n \rangle$  and birefringence ( $\Delta n = n_e - n_o$ ) as [10, 11]:

$$n_e = \langle n \rangle + \frac{2}{3} \Delta n, \quad (4a)$$

$$n_o = \langle n \rangle - \frac{1}{3} \Delta n. \quad (4b)$$

Taking the temperature derivatives of Eq. (4), we obtain the following equations:

$$\frac{dn_e}{dT} = \frac{d\langle n \rangle}{dT} + \frac{2}{3} \frac{d\Delta n}{dT}, \quad (5a)$$

$$\frac{dn_o}{dT} = \frac{d\langle n \rangle}{dT} - \frac{1}{3} \frac{d\Delta n}{dT}. \quad (5b)$$

As will be shown later in the experimental section, the LC average refractive index  $\langle n \rangle$  decreases linearly with increasing temperature for the compounds and mixtures we studied:

$$\langle n \rangle = A - BT, \quad (6)$$

Based on this linear relationship, the first term in Eq. (5) is reduced to a constant  $-B$  for a given LC material. On the other hand, the LC birefringence is linearly proportional to the order parameter  $S$  [12]. Through Haller's semi-empirical equation, the order parameter can be approximated as [13]:

$$S = (1 - T/T_c)^\beta, \quad (7)$$

where  $T$  is the operating temperature,  $T_c$  is the clearing temperature of the LC material, and  $\beta$  is an exponent. For many LC compounds and mixtures studied,  $\beta \sim 0.2$  and is not too sensitive to the LC structures [3]. Thus, the temperature dependant  $\Delta n$  can be rewritten as:

$$\Delta n(T) = (\Delta n)_o (1 - T/T_c)^\beta, \quad (8)$$

In Eq. (8),  $(\Delta n)_o$  stands for the LC birefringence at  $T=0$ K. Substituting Eqs. (6) and (8) back to Eq. (4), we derive the temperature-dependent LC refractive indices:

$$n_e(T) \approx A - BT + \frac{2(\Delta n)_o}{3} \left(1 - \frac{T}{T_c}\right)^\beta, \quad (9a)$$

$$n_o(T) \approx A - BT - \frac{(\Delta n)_o}{3} \left(1 - \frac{T}{T_c}\right)^\beta. \quad (9b)$$

Although there are four parameters in Eq. (9), actually they are obtained by pairs:  $A$  and  $B$  are obtained by fitting the temperature dependent average refractive index  $\langle n \rangle$ , while  $(\Delta n)_o$  and  $\beta$  are obtained by fitting the birefringence data. Taking temperature derivatives of Eq. (9), we derive the following equations:

$$\frac{dn_e}{dT} = -B - \frac{2\beta(\Delta n)_o}{3T_c \left(1 - \frac{T}{T_c}\right)^{1-\beta}} \quad (10a)$$

$$\frac{dn_o}{dT} = -B + \frac{\beta(\Delta n)_o}{3T_c \left(1 - \frac{T}{T_c}\right)^{1-\beta}} \quad (10b)$$

In Eq. (10a), both terms in the right-hand side are negative, independent of temperature. This implies that  $n_e$  decreases as the temperature increases throughout the entire nematic range. However, Eq. (10b) consists of a negative term ( $-B$ ) and a positive term which depends on the temperature. In the low temperature regime ( $T \ll T_c$ ), the positive term could be smaller than the positive term resulting in a negative  $dn_o/dT$ . As the temperature increases, the positive term also increases. As  $T$  approaches  $T_c$ ,  $dn_o/dT$  jumps to a large positive number. In the intermediate, there exists a transition temperature where  $dn_o/dT = 0$ . We define this

temperature as the cross-over temperature  $T_o$  for  $n_o$ . To find  $T_o$ , we simply solve  $dn_o/dT=0$  from Eq. (10b).

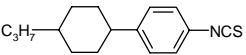
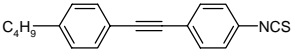
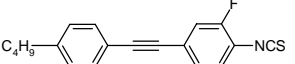
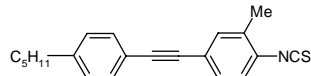
From Eq. (10),  $dn_o/dT$  is determined by five parameters ( $B$ ,  $\beta$ ,  $(\Delta n)_o$ ,  $T$  and  $T_c$ ). Among these five,  $\beta$  and  $T$  can be treated as constants:  $\beta \sim 0.2$  and  $T \sim 295\text{K}$ . Therefore, we only need to consider the remaining three parameters. A smaller  $B$  helps to boost the  $dn_o/dT$  value. Among the LC materials investigated, we found that the compounds containing isothiocyanato (NCS) polar group possess a slightly smaller  $B$  coefficient and higher birefringence than the cyano (CN) compounds. Some experimental evidences will be shown later. Therefore, the remaining two parameters, high birefringence and low clearing temperature, play crucial roles in determining the  $dn_o/dT$  and cross-over temperature. However, these two requirements are often contradicting to each other. Most of the high birefringence LC compounds are associated with high melting and clearing temperatures due to their long molecular conjugation. From Eq. (10b), the  $T_c$  effect is particularly significant. If the  $T_c$  of a LC material is much higher than room temperature, then its cross-over temperature would be relatively high and  $dn_o/dT < 0$  at room temperature. Mixture E7 is such an example; its  $T_c$  is  $60^\circ\text{C}$  and its  $dn_o/dT$  is negative at room temperature.

Although a large positive  $dn_o/dT$  can always be obtained by raising the operating temperature to clearing point, in practice this is undesirable for two reasons. First, in this regime a small temperature fluctuation would cause a large  $dn_o/dT$  change. Second, light scattering due to LC directors fluctuations is strong near the phase transition [14]. Many devices are preferred to operate at room temperature. Thus, it is highly desirable to design a LC mixture exhibiting a large  $dn_o/dT$  at room temperature.

### 3. New mixtures

To design mixtures with high birefringence and low clearing temperature, we selected some laterally substituted isothiocyanato tolanes [15, 16]. Due to the lateral fluoro or methyl substitution, these NCS tolanes exhibit a relatively low clearing temperature. The molecular structures and their corresponding phase transition temperatures (PTT) are listed in Table 1.

Table 1. Molecular structures and phase transition temperatures (PTT) of the compounds used for formulating mixtures. Here, Cr, N, S and I stand for crystalline, nematic, smectic, and isotropic phase, respectively.

LC compounds	Structures	PTT ( $^\circ\text{C}$ )
CP3NCS		Cr 3.0 N 41.3 I
PTP4NCS		Cr 44.0 S <sub>K</sub> 70.5 S <sub>E</sub> 86.9 I
PTP(3F)4NCS		Cr 38.6 I
PTP(3Me)4NCS		Cr 42.3 I

The phase transition temperatures of these LC compounds were measured by using a high sensitivity differential scanning calorimeter (DSC, TA Instrument Model Q-100) at  $2^\circ\text{C}/\text{min}$  scanning rate. By changing the ratio of these single compounds, we prepared two mixtures,

designated as UCF-1 and UCF-2. Their clearing temperatures are 29.7 °C and 32.3 °C, respectively, and melting point below -20 °C. The physical properties of UCF-1 and UCF-2 were measured at room temperature (23°C) and results are listed in Table 2.

Table 2. Physical properties of UCF-1 and UCF-2.  $\Delta n$  was measured at  $\lambda=589$  nm and  $T=23$  °C.

LC Materials	$V_{th}$ (V <sub>rms</sub> )	$\epsilon_{  }$	$\epsilon_{\perp}$	$\Delta\epsilon$	$K_{11}$ (pN)	$K_{33}$ (pN)	$\Delta n$
UCF-1	1.01	13.6	5.2	8.4	4.66	11.4	0.2545
UCF-2	1.15	13.6	4.9	8.7	5.90	11.0	0.2755

#### 4. Results and discussions

We measured the refractive indices of our new mixtures and compared results with three commercial single compounds: 5CB, 6CB, and 5PCH (cyano-chclohexane-phenyl). These LCs are nematic at room temperature and have been used in many LC mixtures. To measure refractive indices, we used a multi-wavelength Abbe refractometer (Atago DR-M4) at  $\lambda=450$ , 486, 546, 589, 633 and 656 nm. The accuracy of the Abbe refractometer is up to the fourth decimal. For a given wavelength, we measured the refractive indices of 5CB, 6CB, UCF-1 and UCF-2 from 10 to 60°C, respectively. The temperature of the Abbe refractometer is controlled by a circulating constant temperature bath (Atago Model 60-C3). The LC molecules are aligned perpendicular to the main prism surface of the Abbe refractometer by coating a surfactant comprising of 0.294 wt% hexadecyletri-methyle-ammonium bromide in methanol solution. Both  $n_e$  and  $n_o$  are obtained through a polarizing eyepiece.

To demonstrate the high  $\Delta n$  advantage, we intentionally designed the UCF-1 and UCF-2 to have similar clearing temperatures as 6CB and 5CB, respectively. Figure 1 depicts the temperature-dependent refractive indices of UCF-1 and 6CB at  $\lambda=589$  nm. Red circles and black triangles represent experimental data for UCF-1 and 6CB, respectively, while solid lines are the fitting results using Eqs. (9a) and (9b). The fitting parameters  $[A, B]$  and  $[(\Delta n)_0, \beta]$  are listed in Table 3. The agreement between experiment and theory is pretty good.

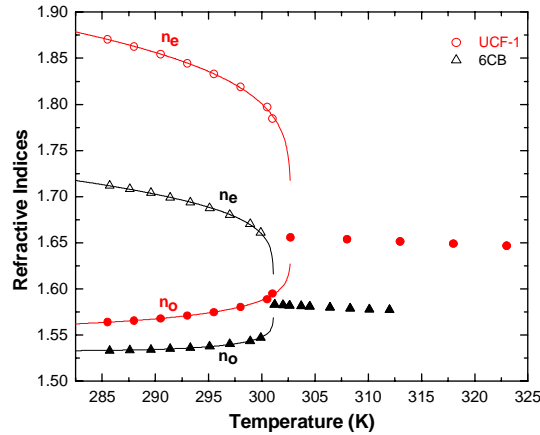


Fig. 1. Temperature-dependent refractive indices of UCF-1 and 6CB at  $\lambda=589$  nm. Red circles and black triangles are refractive indices of UCF-1 and 6CB, respectively. Solid lines are fittings using Eqs. (9a) and (9b). The fitting parameters are listed in Table 3.

From Fig. 1, UCF-1 has a higher  $n_e$ ,  $n_o$  and  $\Delta n$  than 6CB. At room temperature ( $T \sim 295\text{K}$ ), the birefringence of UCF-1 is  $\Delta n \sim 0.25$ , as compared to  $\sim 0.15$  for 6CB. As temperature increases,  $n_e$  decreases while  $n_o$  increases for both UCF-1 and 6CB except at a different rate. The clearing point for UCF-1 and 6CB is 302.7K and 301.1K, respectively. In the isotropic state, the refractive index of UCF-1 and 6CB decreases linearly with increasing temperature. From Fig. 1, we find UCF-1 has a much larger  $dn_o/dT$  than 6CB in the nematic range. We will compare the  $dn_o/dT$  quantitatively for all the LC studied later.

Table 3. Fitting parameters for the average refractive index  $\langle n \rangle$  and birefringence ( $\Delta n$ ) of the five LCs studied: UCF-1, 6CB, UCF-2, 5CB and 5PCH at  $\lambda = 589\text{ nm}$ .

LC Materials	$\langle n \rangle$		$\Delta n$	
	A	B ( $\text{K}^{-1}$ )	$(\Delta n)_o$	$\beta$
UCF-1	1.8112	$5.08 \times 10^{-4}$	0.5397	0.1973
6CB	1.7491	$5.47 \times 10^{-4}$	0.3026	0.1780
UCF-2	1.8100	$4.90 \times 10^{-4}$	0.5416	0.1936
5CB	1.7674	$5.79 \times 10^{-4}$	0.3505	0.1889
5PCH	1.6795	$5.07 \times 10^{-4}$	0.1705	0.1512

Similarly, we prepared UCF-2 to match the clearing temperature of 5CB. The clearing point for UCF-2 and 5CB is 305.3K and 306.4 K, respectively. Figure 2 depicts the temperature-dependent refractive indices of UCF-2 and 5CB at  $\lambda = 589\text{ nm}$ . Magenta circles and blue triangles represent experimental data for UCF-2 and 5CB, respectively, while solid lines are fitting results using Eqs. (9a) and (9b). The fitting parameters  $A$ ,  $B$ ,  $(\Delta n)_o$  and  $\beta$  are also listed in Table 3. From Fig. 2, UCF-2 has a higher  $n_e$ ,  $n_o$  and  $\Delta n$  than 5CB.

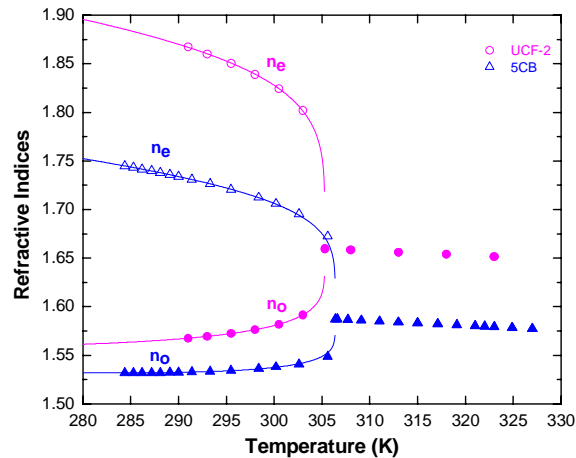


Fig. 2. Temperature-dependent refractive indices of UCF-2 and 5CB at  $\lambda = 589\text{ nm}$ . Magenta circles and blue triangles are refractive indices of UCF-2 and 5CB, respectively, and solid lines are fitting results using Eq. (9). The fitting parameters are listed in Table 3.

To validate Eq. (6), we plot the temperature-dependent average refractive index  $\langle n \rangle$  for UCF-1, UCF-2, 6CB and 5CB at  $\lambda=589$  nm. Results are shown in Fig. 3 where circles represent the experimental data and solid lines are fitting results using Eq. (6). Indeed,  $\langle n \rangle$  decreases linearly as the temperature increases. The fitting parameters  $A$  and  $B$  for these four materials are listed in Table 3.

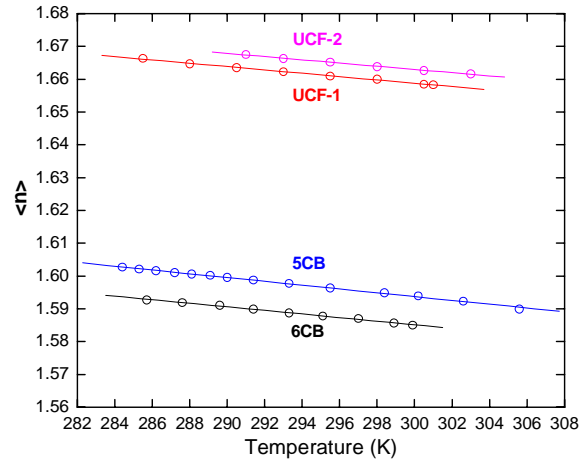


Fig. 3. Temperature-dependent average refractive index of UCF-1, UCF-2, 6CB and 5CB at  $\lambda=589$  nm. Circles represent experimental data and solid lines are fitting results using Eq. (6). The fitting parameters  $A$  and  $B$  for these four materials are listed in Table 3.

Figure 4 depicts the temperature-dependent  $\Delta n$  of UCF-1, UCF-2, 6CB and 5CB at  $\lambda=589$  nm. The circles are experimental data while solid lines are fitting results using Eq. (8). The fitting parameters  $(\Delta n)_0$  and  $\beta$  are listed in Table 3.

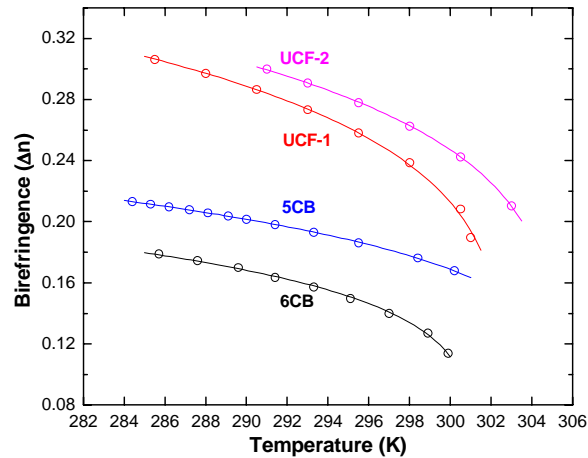


Fig. 4. Temperature-dependent birefringence of UCF-1, UCF-2, 6CB and 5CB at  $\lambda=589$  nm. Red, Magenta, black and blue circles represent experimental data while solid lines are fitting results using Eq. (8). The fitting parameters  $(\Delta n)_0$  and  $\beta$  are listed in Table 3.

Using the parameters listed in Table 3, we are able to calculate the  $dn_e/dT$  and  $dn_o/dT$  for UCF-1, UCF-2, 6CB, 5CB and 5PCH using Eq. (10). Because  $dn_e/dT$  is always negative, we plot  $-dn_e/dT$  instead. Results are shown in Fig. 5 where solid and dashed lines represent the calculated  $dn_o/dT$  and  $-dn_e/dT$  by using Eq. (10) for these five LCs, respectively.

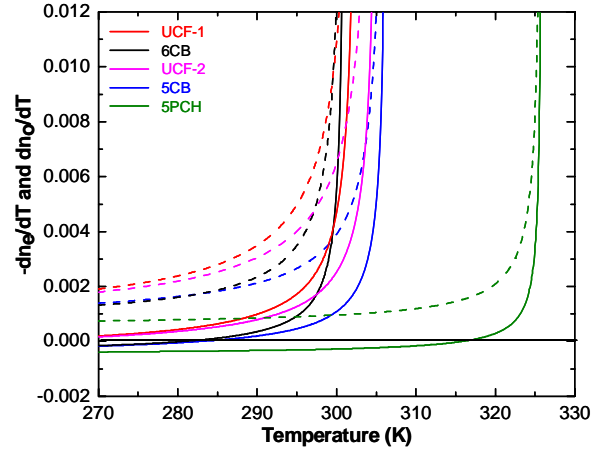


Fig. 5. Temperature-dependent  $dn_o/dT$  of UCF-1, UCF-2, 6CB, 5CB, and 5PCH at  $\lambda=589$  nm. Red, magenta, black, blue and green solid lines represent the calculated  $dn_o/dT$  curves for UCF-1, UCF-2, 6CB, 5CB, and 5PCH, respectively, while the dashed lines represent the calculated  $-dn_e/dT$  curves. The parameters  $B$ ,  $(\Delta n)_o$  and  $\beta$  used in the calculations are listed in Table 3.

From Fig. 5, we find the  $dn_e/dT$  (dashed lines) for both LCs remains negative throughout their nematic range. That means the extraordinary refractive index decreases as the temperature increases in the entire nematic range. However,  $dn_o/dT$  changes sign at the cross-over temperature  $T_o$ . For practical applications, it is desirable to operate the LC device at room temperature (RT). Therefore, we should design a LC with cross-over temperature lower than 295K to assure a positive  $dn_o/dT$  at RT. From Fig. 5, the cross-over temperature ( $T_o$ ) of UCF-1, UCF-2, 6CB, 5CB and 5PCH is  $\sim 254$ K (or  $-19^\circ\text{C}$ ),  $\sim 255$ K (or  $-18^\circ\text{C}$ ),  $\sim 280.8$ K (or  $7.8^\circ\text{C}$ ),  $\sim 282.9$ K (or  $9.9^\circ\text{C}$ ) and  $\sim 315.9$ K (or  $42.9^\circ\text{C}$ ), respectively. Based on Eq. (10b), low  $T_c$  and high birefringence are two important factors for achieving a large  $dn_o/dT$  at RT. The clearing point for UCF-1, UCF-2, 6CB, 5CB and 5PCH is 302.7K, 305.3K, 301.1K, 306.4K, and 326K, respectively. Thus, the  $n_o$  of UCF-1, UCF-2, 6CB, and 5CB increases with increasing temperature when  $T$  is greater than RT but less than  $T_c$ . For 5PCH, its cross-over temperature is higher than RT so that its  $dn_o/dT$  remains negative when  $T < T_o$ . The cross-over temperature we obtained for 5PCH agrees very well with the experimental data reported by the Merck group [17]. As the temperature approaches  $T_c$ , both  $dn_e/dT$  and  $dn_o/dT$  change dramatically as shown clearly in Fig. 5.



The large  $dn_o/dT$  helps to lower the required laser power for observing the thermal soliton effect. From Fig. 5, the  $dn_o/dT$  (in unit of  $K^{-1}$ ) of UCF-1, UCF-2, 6CB and 5CB at RT is  $1.73 \times 10^{-3}$ ,  $1.27 \times 10^{-3}$ ,  $9.24 \times 10^{-4}$ , and  $4.60 \times 10^{-4}$ , respectively. Due to the higher birefringence and a slightly lower clearing temperature, the  $dn_o/dT$  of UCF-1 is ~4X higher than that of 5CB at RT. As  $T$  approaches  $T_c$ , the  $dn_o/dT$  of each LC increases by more than one order of magnitude than that in the nematic phase. However, in the vicinity of phase transition temperature, a small temperature fluctuation would cause a big change in  $dn_o/dT$ . Moreover, light scattering is present in the vicinity of phase transition temperature.

## 5. Conclusion

We have analyzed the factors affecting the  $dn_o/dT$  of a LC material. High birefringence and low clearing temperature are the two most critical parameters. Based on these simple guidelines, we formulated two exemplary high birefringence and low clearing temperature LC mixtures, UCF-1 and UCF-2, using the laterally substituted isothiocyannato tolane compounds. The  $dn_o/dT$  of UCF-1 is about 4X higher than that of 5CB at room temperature. Moreover, the melting temperature of UCF-1 and UCF-2 is below  $-20$  °C, which is much lower than that of 5CB and 6CB. Thus, useful application of these isothiocyannato tolane mixtures for the laser-induced thermal effect is foreseeable.

## Acknowledgments

The authors are indebted to AFOSR for financial support under contract No. F49620-01-1-0377.